

Exact steady state solution of the Boltzmann equation: A driven 1-D inelastic Maxwell gas

A. Santos*

Departamento de Física, Universidad de Extremadura, E-06071 Badajoz, Spain

M. H. Ernst†

*Instituut voor Theoretische Fysica, Universiteit Utrecht,
Postbus 80.195, 3508 TD Utrecht, The Netherlands*

(Dated: November 17, 2018)

The exact nonequilibrium steady state solution of the nonlinear Boltzmann equation for a driven inelastic Maxwell model was obtained by Ben-Naim and Krapivsky [Phys. Rev. E **61**, R5 (2000)] in the form of an infinite product for the Fourier transform of the distribution function $f(c)$. In this paper we have inverted the Fourier transform to express $f(c)$ in the form of an infinite series of exponentially decaying terms. The dominant high energy tail is exponential, $f(c) \simeq A_0 \exp(-a|c|)$, where $a \equiv 2/\sqrt{1-\alpha^2}$ and the amplitude A_0 is given in terms of a converging sum. This is explicitly shown in the totally inelastic limit ($\alpha \rightarrow 0$) and in the quasi-elastic limit ($\alpha \rightarrow 1$). In the latter case, the distribution is dominated by a Maxwellian for a very wide range of velocities, but a crossover from a Maxwellian to an exponential high energy tail exists for velocities $|c - c_0| \sim 1/\sqrt{q}$ around a crossover velocity $c_0 \simeq \ln q^{-1}/\sqrt{q}$, where $q \equiv (1-\alpha)/2 \ll 1$. In this crossover region the distribution function is extremely small, $\ln f(c_0) \simeq q^{-1} \ln q$.

PACS numbers: 45.70.-n, 05.20.Dd, 51.10.+y

I. INTRODUCTION

In kinetic theory there is a long standing interest in overpopulated high energy tails of velocity distribution functions [1] because of chemical reactions and other activated processes that occur only at energies far above thermal. This interest has been considerably increased in the past 10 years because of research in granular fluids with dissipative or inelastic interactions. The velocity distributions in fluidized systems have been studied theoretically [2, 3, 4, 5, 6, 7, 8], and measured in Monte Carlo [8, 9, 10] and molecular dynamics simulations [11], and in numerous laboratory experiments [12].

Very recently a revival in this field occurred when Baldassarri et al. [13, 14] discovered an exact scaling solution – with an algebraic high energy tail – of the non-linear Boltzmann equation for an inelastic one-dimensional freely cooling gas (without energy input) with a collision frequency independent of the energy of the colliding particles. This model, called Inelastic Maxwell Model (IMM), was introduced by Ben-Naim and Krapivsky [15]. It is in fact an inelastic modification of Ulam’s stochastic model to illustrate the velocity relaxation of elastic one-dimensional point particles towards a Maxwellian [16]. A three-dimensional version of it has been constructed by Bobylev et al. [17, 18]. For a recent review on inelastic Maxwell models, see Refs. [19, 20].

Baldassarri et al. have demonstrated the importance of

this type of solutions in [13] with the help of Monte Carlo simulations of the nonlinear Boltzmann equation for 1-dimensional and 2-dimensional IMM’s. It appeared that the solution, $F(v, t)$, for large classes of initial distributions $F(v, 0)$ (e.g. uniform or Gaussian) and for all values of the inelasticity could be collapsed for large times on a scaling form $v_0^{-d}(t)f(v/v_0(t))$, where $v_0(t) = \langle v^2 \rangle^{1/2}$ is the r.m.s. velocity. In one dimension the scaling form was given by $f(c) = (2/\pi)(1+c^2)^{-2}$, which has a heavily overpopulated algebraic tail $\sim c^{-4}$ when compared to a Maxwellian. In two dimensions the solutions also approached a scaling form with an algebraic tail, $f(c) \sim c^{-d-a}$ with an exponent $a(q)$ that depends on the degree of inelasticity $q = \frac{1}{2}(1-\alpha)$, where α is the coefficient of restitution. Soon after, Ben-Naim and Krapivsky [21], and Ernst and Brito [22] obtained asymptotic solutions with algebraic tails for the velocity distribution in d -dimensional freely cooling IMM’s from self-consistently determined solutions of the Boltzmann equation. Using methods previously developed for the inelastic hard sphere case, the asymptotic solutions were also extended to non-equilibrium steady states (NESS) in d -dimensional systems driven by Gaussian white noise and other thermostats [5, 23]. There the tails exhibited over-populations of exponential type, $\sim \exp(-a|c|)$, for all d -dimensional IMM’s [23]. For inelastic hard spheres, which is the prototypical model for granular gases, the velocity distribution function shows an overpopulated exponential tail in free cooling [5, 8, 9], and a stretched exponential tail $\sim \exp(-a|c|^{3/2})$, when driven by white noise [5, 8, 10].

For the case of d -dimensional free IMM’s the approach of $F(v, t)$ to a scaling form with an algebraic tail has also been rigorously proven, for initial distributions in the \mathcal{L}_1

*Electronic address: andres@unex.es

†Electronic address: ernst@phys.uu.nl

function space, satisfying the physical requirements of finite mass and energy, i.e. $\int d\mathbf{v}\{1, v^2\}F(v, 0) < \infty$ [24].

What about exact and/or more explicit results for the distribution function in the one-dimensional IMM, driven by Gaussian white noise? The exact solution of the nonlinear Boltzmann equation for this case is given in the form of an infinite product for the Fourier transform of the distribution function [15]. Nienhuis and van der Hart [25] made an extensive numerical analysis of this solution, and demonstrated exponential decay, in agreement with the predictions of Ref. [23]. More numerical evidence for exponential high energy tails in the one-dimensional driven IMM was given recently by Marconi and Puglisi [26], and by Antal et al. [27]. In a recent paper [20], Ben-Naim and Krapivsky have also used the Fourier transform method to show that the high energy tail is exponential for any inelasticity, but with an amplitude that diverges in the quasi-elastic limit. On the other hand, the problem of determining for what range of velocities the exponential tail actually applies remains open. This is one of the points addressed in this paper.

The plan of the paper is as follows. In the remainder of this Section we present the nonlinear Boltzmann equation for the velocity distribution function $F(v)$ or $f(c)$, driven by Gaussian white noise, and we discuss qualitatively the physical properties of the model in different limiting cases. In Section II the exact solution $\phi(k) = \int dc e^{-ikc} f(c)$ of the Fourier transformed Boltzmann equation in the NESS is presented in the form of an infinite product, and its large- and small- k properties are analyzed. In Section III we determine the inverse Fourier transform, $f(c)$, in the form of an infinite series of exponentially decaying terms. In the limit of totally inelastic collisions ($\alpha \rightarrow 0$) substantial simplifications occur. The rather singular quasi-elastic limit ($\alpha \rightarrow 1$) is studied in Section IV, where also the crossover from Maxwellian to exponential decay is analyzed. We end with some comments in Section V, and some technical details are moved to Appendices A and B.

Before concluding this introduction we present the Boltzmann equation for the one-dimensional inelastic Maxwell model (IMM) [15], driven by Gaussian white noise, and we discuss some of its important properties. The time evolution of a spatially homogeneous isotropic velocity distribution function $F(v, t) = F(|v|, t)$ is described by the nonlinear Boltzmann equation ,

$$\begin{aligned} \frac{\partial F(v)}{\partial t} - D \frac{\partial^2 F(v)}{\partial v^2} &= \int dv_1 \left[\frac{1}{\alpha} F(v'') F(v_1'') - F(v) F(v_1) \right] \\ &= -F(v) + \frac{1}{p} \int du F(u) F\left(\frac{v-qu}{p}\right) \equiv I(v|F). \end{aligned} \quad (1.1)$$

All velocity integrations extend over the interval $(-\infty, +\infty)$. The diffusion term represents the (heating) effect of the Gaussian white noise with noise strength D . The nonlinear collision term represents the inelastic collisions, where $v'' = v - \frac{1}{2}(1 + \alpha^{-1})(v - v_1)$ and $v_1'' = v_1 + \frac{1}{2}(1 + \alpha^{-1})(v - v_1)$ denote restituting velocities. Here $\alpha = 2p - 1 = 1 - 2q$ with $0 < \alpha < 1$ is the coefficient of restitution. The mass is normalized as

$\int dv F(v) = 1$, and the mean square velocity or temperature as $\langle v^2 \rangle(t) = \int dv v^2 F(v) \equiv v_0^2(t)$. The rate equation,

$$\partial_t \langle v^2 \rangle = 2D - 2pq \langle v^2 \rangle, \quad (1.2)$$

obtained from (1.1), describes the approach to the non-equilibrium steady state (NESS) with width $\langle v^2 \rangle = D/pq$, where the heating rate D caused by the random forces is balanced by the loss rate, $pq \langle v^2 \rangle = \frac{1}{4}(1 - \alpha^2) \langle v^2 \rangle$, caused by the inelastic collisions.

To understand the physical processes involved, we first discuss in a qualitative way the relevant limiting cases. Without the heating term ($D = 0$), Eq. (1.1) reduces to the freely cooling IMM, whose exact solution has been discussed in Refs. [13, 14]. If one takes in addition the elastic limit ($\alpha \rightarrow 1$ or $q \rightarrow 0$), the collision laws reduce in the *one-dimensional* case to $v'' = v_1, v_1'' = v$, i.e. an exchange of particle labels, the collision term vanishes identically, every $F(v, t) = F(v)$ is a solution, there is no randomization or relaxation of the velocity distribution through collisions, and the model becomes trivial at the Boltzmann level of description, whereas the distribution function in the presence of *infinitesimal* dissipation ($\alpha \rightarrow 1$) approaches a Maxwellian.

If we turn on the noise ($D \neq 0$) at vanishing dissipation ($q = 0$), the exact solution of (1.1) in Fourier representation is $\widehat{F}(k, t) = \exp(-Dk^2 t) \widehat{F}(k, 0)$, and the granular temperature, $v_0^2(t) = v_0^2(0) + 2Dt$, increases linearly with time. With stochastic heating *and* dissipation (even in infinitesimal amounts) the system reaches a NESS, and it is the goal of this paper to determine the NESS distribution function.

To expose the universality of this NESS it is convenient to measure the velocities, $c = v/v_0(\infty)$, in units of its typical size $v_0(\infty)$, i.e. the r.m.s. velocity or width of the velocity distribution $v_0(\infty)$,

$$F(v, \infty) = v_0^{-1}(\infty) f(v/v_0(\infty)), \quad (1.3)$$

which obeys the normalizations $\int dc \{1, c^2\} f(c) = \{1, 1\}$. Different normalizations have been used as well [28].

The rescaled velocity distribution in the NESS is then the solution of the scaling equation,

$$I(c|f) = -\frac{D}{v_0^2(\infty)} f''(c) = -pq f''(c), \quad (1.4)$$

where primes denote c -derivatives. The first equality may suggest that $f(c)$ may depend on the noise strength D and possibly on the initial distribution via $v_0(\infty)$. By eliminating $v_0(\infty)$ with the help of (1.2) in the NESS we have shown that the scaling form of the distribution function $f(c)$ is a *universal* function, that does not depend on the strength D of this thermostat, nor on any property of the initial distribution. It only depends on the type of thermostat used.

II. FOURIER TRANSFORM OF IMM BOLTZMANN EQUATION

The nonlinear Boltzmann equation for characteristic function, $\phi(k) = \int dc e^{-ikc} f(c)$, is obtained by Fourier transformation of (1.4) with the result,

$$(1 + pqk^2)\phi(k) = \phi(pk)\phi(qk). \quad (2.1)$$

The simple structure of the equation for the Fourier transform $\phi(k)$ follows because the nonlinear collision operator for (in)elastic Maxwell models is a convolution in the velocity variables [1]. Equation (2.1) is a nonlinear finite difference equation, that can be solved by iteration. A simple way to construct the exact solution is to introduce $\psi(k) \equiv \ln \phi(k)$, which satisfies

$$\psi(k) = \psi(pk) + \psi(qk) - \ln(1 + pqk^2). \quad (2.2)$$

The normalization of mass and energy implies that $\phi(k) \approx 1 - \frac{1}{2}k^2$ and $\psi(k) \approx -\frac{1}{2}k^2$ at small k . The solution to (2.2) can be found iteratively starting from $\psi_0(k) = -\ln(1 + pqk^2)$ and inserting $\psi_n(k)$ on the right-hand-side of (2.2) to get $\psi_{n+1}(k)$ on the left-hand-side. By taking the limit $\psi(k) = \lim_{n \rightarrow \infty} \psi_n(k)$, one finally obtains,

$$\begin{aligned} \psi(k) &= - \sum_{m=0}^{\infty} \sum_{\ell=0}^m \nu_{m\ell} \ln \left[1 + p^{2\ell} q^{2(m-\ell)} pqk^2 \right] \\ \phi(k) &= \prod_{m=0}^{\infty} \prod_{\ell=0}^m [1 + p^{2\ell} q^{2(m-\ell)} pqk^2]^{-\nu_{m\ell}}, \end{aligned} \quad (2.3)$$

where $\nu_{m\ell} = \binom{m}{\ell}$. These solutions satisfy the required boundary conditions at $k = 0$. We further note that $\bar{\psi}(k) = \psi(k) - \lambda|k|$ with λ an arbitrary complex number is also a solution of (2.2), but in general does not satisfy the boundary conditions at small k . This property is a reflection of the Galilean invariance of the original Boltzmann equation.

Equations (2.3) provide an exact representation in Fourier space of the solution of the Boltzmann equation (1.1). The series (2.3) converges rapidly, even for large k . By expanding the logarithm in powers of k^2 and summing a geometric series we obtain,

$$\psi(k) = \sum_{n=1}^{\infty} \frac{(-1)^n}{n} \frac{(k^2 pq)^n}{1 - p^{2n} - q^{2n}}. \quad (2.4)$$

It converges for $k^2 \leq 1/pq$, and $\psi(k)$ has a branch point singularity at $k^2 = -1/pq$, as is apparent from (2.2). Equation (2.4) allows one to get the cumulants C_{2n} defined by

$$\psi(k) = \sum_{n=1}^{\infty} \frac{(-1)^n}{(2n)!} C_{2n} k^{2n}, \quad (2.5)$$

with the result

$$C_{2n} = \frac{(2n)!}{n} \frac{(pq)^n}{1 - p^{2n} - q^{2n}}. \quad (2.6)$$

In particular, $C_2 = \langle c^2 \rangle = 1$. Since $1 - p^{2n} - q^{2n} > 0$, it follows that *all* cumulants are positive, indicating already an overpopulation of the high energy tails. So far a summary of the results obtained in Ref. [15]. We note that the Stirling approximation shows that the cumulants at fixed α or q and $n > e/(2\sqrt{pq})$ are rapidly diverging with increasing n , as $C_{2n} \sim 2\sqrt{\pi/n}(2n\sqrt{pq}/e)^{2n}$.

The exact solution $\phi(k)$ in (2.3) has an infinite sequence of poles of multiplicity $\nu_{m\ell}$ in the complex k -plane, all of which contribute to the amplitude of the asymptotic high energy tail of $f(c)$. This makes a numerical inversion of $\phi(k)$ to obtain $f(c)$ a bit tricky. To determine $f(c)$ several authors [25, 27] have performed numerical inversions of $\phi(k)$, starting from the infinite product (2.3) or from the more convenient series expansion (2.4). However the latter one is only convergent for $pqk^2 < 1$. To facilitate such numerical procedures, we have derived an expansion in powers of k^{-2} , convergent in the complementary region, $pqk^2 > 1$, of the complex k -plane. This rather technical part is deferred to Appendix A. The results can be found in (A2), (A4), and (A7).

III. HIGH ENERGY TAIL

On account of (2.3), the characteristic function $\phi(k)$ can be written as

$$\phi(k) = \prod_{m=0}^{\infty} \prod_{\ell=0}^m (1 + k^2/k_{m\ell}^2)^{-\nu_{m\ell}}, \quad (3.1)$$

where $k_{m\ell} \equiv ap^{-\ell}q^{-(m-\ell)}$ with $a \equiv 1/\sqrt{pq}$. Thus $\phi(k)$ has poles at $k = \pm ik_{m\ell}$ with multiplicity $\nu_{m\ell}$. The velocity distribution,

$$f(c) = \frac{1}{2\pi} \int_{-\infty}^{\infty} dk e^{ikc} \phi(k), \quad (3.2)$$

can then be obtained by contour integration. As $f(c)$ is an even function, we only need to evaluate the integral in (3.2) for $c > 0$. The replacement $c \rightarrow |c|$ gives then the result for all c . By closing the contour through an infinite upper half-circle and applying the residue theorem we obtain

$$f(c) = \sum_{m=0}^{\infty} \sum_{\ell=0}^m e^{-k_{m\ell}|c|} \sum_{n=0}^{\nu_{m\ell}-1} |c|^n A_{m\ell n}, \quad (3.3)$$

where

$$\begin{aligned} A_{m\ell n} &= \frac{i^{n+1} k_{m\ell}^{2\nu_{m\ell}}}{n!(\nu_{m\ell} - 1 - n)!} \lim_{k \rightarrow ik_{m\ell}} \left(\frac{\partial}{\partial k} \right)^{\nu_{m\ell} - 1 - n} \\ &\quad \times (k + ik_{m\ell})^{-\nu_{m\ell}} \tilde{\phi}_{m\ell}(k), \end{aligned} \quad (3.4)$$

with

$$\tilde{\phi}_{m\ell}(k) \equiv \prod_{m'=0}^{\infty} \prod_{\ell'=0}^{m'} (1 + k^2/k_{m'\ell'}^2)^{-\nu_{m'\ell'}(1 - \delta_{mm'}\delta_{\ell\ell'})}. \quad (3.5)$$

Note that the factor labeled $(m', \ell') = (m, \ell)$ is absent. The dominant terms in (3.3) for large $|c|$ correspond to the smallest values of $k_{m\ell}$. The two smallest ones are $k_{00} = a$ and $k_{11} = a/p$. Consequently, the leading and sub-leading terms are

$$f(c) \approx A_0 e^{-a|c|} + A_1 e^{-a|c|/p} + \dots, \quad (3.6)$$

where

$$A_n \equiv A_{nn0} = (a/2p^n) \tilde{\phi}_{nn}(ia/p^n). \quad (3.7)$$

We calculate the first two explicitly, i.e.

$$A_0 = \frac{a}{2} \exp \left[\sum_{m=1}^{\infty} \frac{p^{2m} + q^{2m}}{m(1-p^{2m} - q^{2m})} \right] \quad (3.8)$$

$$A_1 = \frac{-ap^3}{2(1-p^2)(p-q)} \times \exp \left[\sum_{m=1}^{\infty} \frac{p^{-2m}(p^{2m} + q^{2m})^2}{m(1-p^{2m} - q^{2m})} \right]. \quad (3.9)$$

In the last equalities we have followed steps similar to those used to obtain (2.4) from (2.3). The results (3.3)–(3.9) exhibit the full analytic structure of the dominant and subdominant high energy tails of the velocity distribution in the NESS, as already demonstrated numerically for the one-dimensional case in Refs. [25, 26, 27], and derived in [23] for d -dimensional IMM's on the basis of self-consistent solutions. Moreover we have obtained here explicit expressions for the amplitudes A_0 and A_1 in the form of sums that are rapidly converging when q is not too small. The coefficients $A_0 \equiv A_{000}$ and $A_1 \equiv A_{110}$ are shown in Fig. 1 as functions of α , where $A_{110} \propto 1/(p-q) = 1/\alpha$ diverges according to (3.9). The next term to those explicitly given in (3.6) corresponds either to $k_{22} = a/p^2$ if $p^2 > q$ (i.e., if $\alpha > \sqrt{5} - 2 \simeq 0.236$) or to $k_{10} = a/q$ if $p^2 < q$. Note that the amplitude A_{100} of $\exp(-k_{10}|c|)$ can be obtained from A_1 in (3.9) by interchanging $p \leftrightarrow q$. Figure 2 compares the asymptotic form $f(c) \approx A_0 e^{-a|c|}$ with the function $f(c)$ obtained by numerically inverting $\phi(k)$ for $\alpha = 0$ and $\alpha = 0.5$. We observe that the asymptotic behavior is reached for $a|c| \gtrsim 4$ if $\alpha = 0$ and for $a|c| \gtrsim 8$ if $\alpha = 0.5$. As $a = 1/\sqrt{pq}$ this corresponds to velocities far above the r.m.s. velocity.

There are two interesting limiting cases: the *quasi-elastic* limit ($\alpha \rightarrow 1, q \rightarrow 0$), and the *totally inelastic* limit ($\alpha \rightarrow 0, p \rightarrow \frac{1}{2}^+, q \rightarrow \frac{1}{2}^-$). We start with the latter. In the totally inelastic limit ($\alpha \rightarrow 0$) the subdominant terms $A_{110} e^{-a|c|/p}$ and $A_{100} e^{-a|c|/q}$ become equally important, i.e. the single poles in (3.1) at $k_{11} = a/p$ and $k_{10} = a/q$ coalesce, and (3.6) no longer describes the subdominant large- c behavior correctly. Moreover $A_{110} \simeq -A_{100} \propto 1/\alpha$, as can be seen in Fig. 1 for A_{110} . In fact, the poles $k_{m\ell} \rightarrow k_m \equiv 2^m a$ coalesce for all ℓ , some of the coefficients $A_{m\ell n}$ diverge, e.g. $A_{mm0} \propto (1/\alpha)^{2^m - 1}$, and the expansion makes no sense anymore. So, we an-

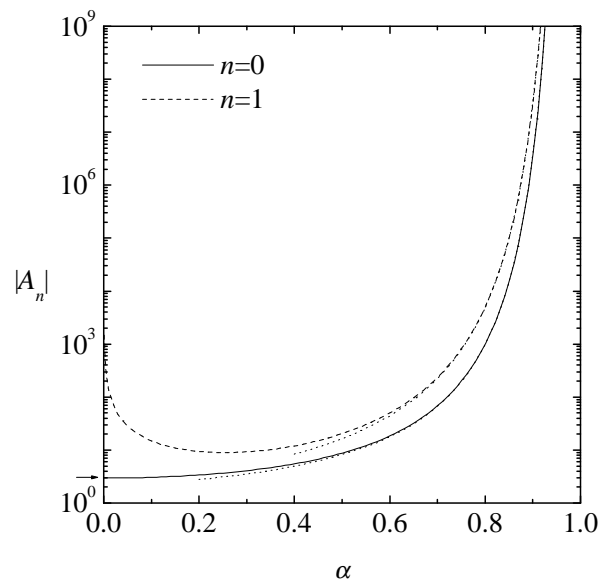


FIG. 1: Logarithmic plot of the amplitudes $A_0 \equiv A_{000}$ (solid line) and $-A_1 \equiv -A_{110}$ (dashed line) as functions of the coefficient of restitution. The arrow indicates the value $A_0 \simeq 2.958389$ at $\alpha = 0$. The dotted lines represent the asymptotic form (4.11) for small q .

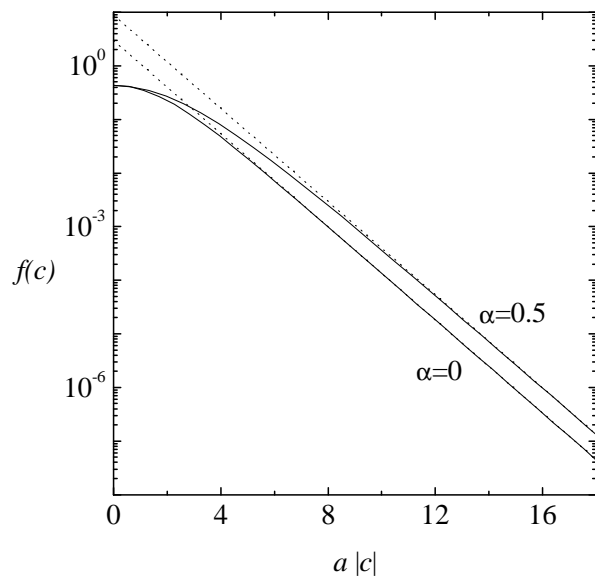


FIG. 2: Logarithmic plot of $f(c)$ versus $a|c|$ for $\alpha = 0$ and $\alpha = 0.5$. The dotted lines are the asymptotic forms $f(c) \approx A_0 e^{-a|c|}$ at $\alpha = 0$ and $\alpha = 0.5$, with A_0 obtained from (3.8).

alyze the case $\alpha = 0$ separately. In this case the characteristic function is according to (2.3),

$$\phi(k) = \prod_{m=0}^{\infty} (1 + k^2/k_m^2)^{-\nu_m}, \quad (3.10)$$

where $\nu_m \equiv 2^m$ and $k_m \equiv 2^m a$ with $a = 1/\sqrt{pq} = 2$.

Then the distribution function is

$$f(c) = \sum_{m=0}^{\infty} e^{-k_m|c|} \sum_{n=0}^{\nu_m-1} |c|^n A_{mn}, \quad (3.11)$$

where the residues or amplitudes are given by,

$$A_{mn} = \frac{i^{n+1} k_m^{2\nu_m}}{n!(\nu_m - 1 - n)!} \lim_{k \rightarrow ik_m} \left(\frac{\partial}{\partial k} \right)^{\nu_m-1-n} \times (k + ik_m)^{-\nu_m} \tilde{\phi}_m(k), \quad (3.12)$$

and $\tilde{\phi}_n(k)$ is defined as,

$$\tilde{\phi}_n(k) \equiv \prod_{m=0}^{\infty} (1 + k^2/k_m^2)^{-\nu_m(1-\delta_{nm})}. \quad (3.13)$$

For large $|c|$ the distribution function becomes,

$$f(c) \approx A_{00} e^{-2|c|} + (A_{10} + A_{11}|c|) e^{-4|c|} + \dots \quad (3.14)$$

To calculate the amplitudes of the dominant terms we derive from (3.13),

$$\begin{aligned} \ln \tilde{\phi}_0(k) &= - \sum_{m=1}^{\infty} 2^m \ln(1 + 2^{-2m} k^2/a^2) \\ &= \sum_{n=1}^{\infty} \frac{(-1)^n}{n} \frac{(k/a)^{2n}}{2^{2n-1} - 1} \\ \ln \tilde{\phi}_1(k) &= - \ln(1 + k^2/a^2) \\ &\quad + 2 \sum_{n=1}^{\infty} \frac{(-1)^n}{n} \frac{(k/2a)^{2n}}{2^{2n-1} - 1}. \end{aligned} \quad (3.15)$$

The definitions (3.12)–(3.13) with $k_m = 2^m a$ ($a = 2$) yield then,

$$\begin{aligned} A_{00} &= \frac{1}{2} a \tilde{\phi}_0(ia) = e^{S_0} \simeq 2.958389 \\ A_{11} &= a^2 \tilde{\phi}_1(2ia) = -\frac{4}{3} A_{00}^2 \simeq -11.669422 \\ A_{10} &= \frac{1}{2} a \tilde{\phi}_1(2ia) - ia^2 \tilde{\phi}'_1(2ia) \\ &= \frac{4}{3} (S_1 - \frac{11}{12}) A_{00}^2 \simeq 3.138267, \end{aligned} \quad (3.16)$$

where we have used the rapidly converging sums,

$$\begin{aligned} S_0 &= \sum_{n=1}^{\infty} \frac{1}{n} (2^{2n-1} - 1)^{-1} \simeq 1.084645 \\ S_1 &= \sum_{n=1}^{\infty} (2^{2n-1} - 1)^{-1} \simeq 1.185597. \end{aligned} \quad (3.17)$$

In fact, the results (3.14) could have been derived directly from (3.3)–(3.9) after lengthy calculations, by expanding A_{110} and A_{100} in powers of α , with the result,

$$A_{1s0} = (-1)^{s+1} A_{11}/(8\alpha) + \frac{1}{2} A_{10} + \mathcal{O}(\alpha) \quad (3.18)$$

with $s = 0, 1$. Insertion of these results in (3.3) yields (3.14). The limit $\alpha \rightarrow 1$ is discussed in the next Section.

IV. QUASI-ELASTIC LIMIT

As already mentioned in the introduction, the velocity distribution approaches a NESS, even in the presence of an *infinitesimal* dissipation ($\alpha \rightarrow 1, q \rightarrow 0$), balanced by a ditto amount of stochastic heating. This limit is referred to as the quasi-elastic limit. For the rescaled functions $f(c)$ and $\phi(k)$ it simply refers to the limit $q \rightarrow 0$.

Once we have *first* taken the large $|c|$ limit at *fixed* $\alpha < 1$ — as has been done in the previous Section — we can *next* take the quasi-elastic limit $\alpha \rightarrow 1$. When the limits are taken in that order, the asymptotic behavior is still of the form $e^{-a|c|}$, where the decay constants are $k_{mm} = a/p^m \rightarrow a$, and the amplitudes may diverge. On the other hand, if the limits are taken in the reverse order, *first* $\alpha \rightarrow 1$ at *fixed* $|c|$ and *next* $|c| \rightarrow \infty$, the behavior is in general totally different.

First consider the second case, and observe that $\psi(k)$ in (2.4) has at small q the form $\psi(k) = -\frac{1}{2}k^2 + \sum_{n=2}^{\infty} a_{2n}(q)k^{2n}$ with rapidly decreasing coefficients $a_{2n} \simeq (-1)^n q^{n-1} (1 - \frac{1}{2}q)/(2n^2)$ for $n \geq 2$. Consequently $\phi(k) = e^{\psi(k)}$ can be expanded as,

$$\phi(k) = e^{-\frac{1}{2}k^2} \left[1 + \sum_{n=2}^{\infty} \mu_{2n}(q) k^{2n} \right], \quad (4.1)$$

where the relation between a_{2n} and μ_{2n} is the same as between cumulants and moments after setting $a_2 = \mu_2 = 0$. The coefficients μ_{2n} are to dominant order in q^2 given by

$$\begin{aligned} \mu_4 &= a_4 = \frac{1}{8}q(1 - \frac{1}{2}q - \frac{3}{4}q^2) + \mathcal{O}(q^4) \\ \mu_6 &= a_6 = -\frac{1}{18}q^2(1 - \frac{1}{2}q) + \mathcal{O}(q^4) \\ \mu_8 &= \frac{1}{2}a_4^2 + a_8 = \frac{1}{128}q^2(1 + 3q) + \mathcal{O}(q^4) \\ \mu_{10} &\simeq a_4 a_6 = -\frac{1}{144}q^3 + \mathcal{O}(q^4) \\ \mu_{12} &\simeq \frac{1}{6}a_4^3 = \frac{1}{3072}q^3 + \mathcal{O}(q^4), \end{aligned} \quad (4.2)$$

and in general $\mu_{4n-2} \sim \mu_{4n} \sim \mathcal{O}(q^n)$ for $n \geq 2$. The series above can be Fourier inverted term-wise, using the following relation,

$$\begin{aligned} \int_{-\infty}^{\infty} \frac{dk}{2\pi} e^{ikc} e^{-\frac{1}{2}k^2} k^{2n} &= (-1)^n \left(\frac{d}{dc} \right)^{2n} \exp(-\frac{1}{2}c^2)/\sqrt{2\pi} \\ &= (-1)^n He_{2n}(c) f_0(c) = 2^n n! L_n^{(-1/2)}(\frac{1}{2}c^2) f_0(c), \end{aligned} \quad (4.3)$$

where $f_0(c) = \exp(-\frac{1}{2}c^2)/\sqrt{2\pi}$ is the Maxwellian. In the last two equalities Rodrigues' formula for the Hermite polynomials has been used, as well as their relation to the generalized Laguerre or Sonine polynomials (see Ref. [29], Eqs. (22.11.88), (22.5.18) and (22.5.40)). The resulting Sonine polynomial expansion of the velocity distribution in the NESS reads then,

$$f(c) = f_0(c) \left[1 + \sum_{n=2}^{\infty} (-1)^n \mu_{2n}(q) He_{2n}(c) \right]. \quad (4.4)$$

Similar expansions of the NESS-distribution function in low order Hermite or Sonine polynomials have also been

derived for inelastic hard spheres in d -dimensions [5], and for a 3-dimensional IMM in [18].

Next we consider the case, where *first* $|c| \rightarrow \infty$ at finite $\alpha < 1$, and *next* $\alpha \rightarrow 1$, or $q \rightarrow 0$. The large- c behavior at fixed α has already been discussed in (3.3)–(3.9), and we observe that the terms in Eq. (3.3) at large c , associated with all poles of the form $k_{n\ell} = a/p^\ell q^{n-\ell}$ ($\ell < n$) decay rapidly as $q \rightarrow 0$, and only poles with $k_{nn} = a/p^n$ need to be considered:

$$f(c) = \sum_{n=0}^{\infty} A_n e^{-k_{nn}|c|}. \quad (4.5)$$

We will analyze the behavior of the associated amplitudes A_n by combining (3.7) with (3.5), i.e.

$$\begin{aligned} \ln A_n &= \ln(a/2p^n) \\ &- \sum_{m=0}^{\infty} \sum_{\ell=0}^m \binom{m}{\ell} (1 - \delta_{mn} \delta_{\ell n}) \ln [1 - p^{-2(n-\ell)} q^{2(m-\ell)}] \\ &\equiv B_n^{(1)} + B_n^{(2)} + B_n^{(3)} + \ln(a/2p^n), \end{aligned} \quad (4.6)$$

where

$$\begin{aligned} B_n^{(1)} &= - \sum_{m=0}^{n-1} \sum_{\ell=0}^m \binom{m}{\ell} \ln [1 - p^{-2(n-\ell)} q^{2(m-\ell)}] \\ B_n^{(2)} &= - \sum_{\ell=0}^{n-1} \binom{n}{\ell} \ln [1 - (q/p)^{2(n-\ell)}] \\ B_n^{(3)} &= - \sum_{m=n+1}^{\infty} \sum_{\ell=0}^m \binom{m}{\ell} \ln [1 - p^{-2(n-\ell)} q^{2(m-\ell)}]. \end{aligned} \quad (4.7)$$

Now we take the limit $q \rightarrow 0$ at *finite* n and retain terms to order q . The dominant small- q contribution to $B_n^{(1)}$ comes from $\ell = m$, i.e.

$$\begin{aligned} B_n^{(1)} &= - \sum_{m=1}^n \ln (1 - p^{-2m}) + o(q) \\ &= - \ln [(-2q)^n n!] - \frac{1}{2} n(n+2)q + o(q), \end{aligned} \quad (4.8)$$

where we used the relation $1 - 1/p^{2m} \simeq -2mq[1 + (m + \frac{1}{2})q]$, and $o(q^k)$ denotes terms which are negligible with respect to q^k . Note that the complex number $B_n^{(1)}$ is only determined modulo $\{2\pi i\}$, but $\exp(B_n^{(1)})$ is single-valued. Furthermore, we observe that $B_n^{(2)} = \mathcal{O}(nq^2)$. The analysis of $B_n^{(3)}$ in (4.7) is more involved and given in Appendix B. The result is,

$$B_n^{(3)} = \frac{\pi^2}{12q} + \frac{1}{2} \ln q - K_0 + \frac{1}{2} \left(n + \frac{13}{12} - \frac{\pi^2}{72} \right) q + o(q), \quad (4.9)$$

where

$$K_0 = \frac{3}{4} + \frac{\pi^2}{24} - \frac{1}{2} \ln 2 - R \simeq 0.733598. \quad (4.10)$$

Combining the small- q results (4.8) and (4.9) for $B_n^{(1)}$ and $B_n^{(3)}$ with (4.6) yields for A_n ,

$$\begin{aligned} A_n &= \frac{a}{2p^n} \exp [B_n^{(1)} + B_n^{(3)} + o(q)] \\ &= \frac{(-1)^n}{2n!(2q)^n} \exp \left[\frac{\pi^2}{12q} - K_0 - \frac{1}{2} n(n-1)q + K_1 q + o(q) \right], \end{aligned} \quad (4.11)$$

where

$$K_1 = \frac{25}{24} - \frac{\pi^2}{144} \simeq 0.9731278. \quad (4.12)$$

To describe the crossover between the two different limiting behaviors, i.e. (4.4) with first $q \rightarrow 0$, next $c \rightarrow \infty$, and (4.5), (4.11) with first $c \rightarrow \infty$, next $q \rightarrow 0$ we need to couple these limits, which will be discussed next.

By an extension of the steps followed in Appendix B, it can be verified that the terms denoted by $o(q)$ in Eq. (4.11) have the form $n^{k_1} q^{k_2}$ with $k_1 \leq k_2 + 1$ and $k_2 \geq 2$. Therefore, those terms can be neglected against the terms of order q if $n \ll q^{-1}$.

The ratio $R(c)$ between the distribution function $f(c)$ in (4.5) and its asymptotic high energy form $A_0 e^{-a|c|}$, defines a *crossover* function

$$R(c) \equiv f(c)/A_0 e^{-a|c|} = \sum_{n=0}^{\infty} b_n r_n, \quad (4.13)$$

where r_n and $b_n = A_n/A_0$ follow from (4.5) and (4.11) as,

$$\begin{aligned} r_n &= \exp [-a|c|(p^{-n} - 1)] \\ b_n &= \frac{(-1)^n}{n!(2q)^n} \exp [-\frac{1}{2} n(n-1)q + o(n^2 q)]. \end{aligned} \quad (4.14)$$

Here we have written $o(q) \rightarrow o(n^2 q)$ to emphasize the fact that Eq. (4.14) remains valid if $n \ll q^{-1}$. So there is a crossover behavior in $R(c)$ from a large- c behavior of $\mathcal{O}(\exp[-c^2/2]) \simeq 0$ in the small- q Sonine polynomial expansion (3.4), to the the small- q behavior of $R(c)$ of $\mathcal{O}(1)$ in (4.13). The transition region is characterized by a crossover velocity c_0 such that $R(c_0) \approx \frac{1}{2}$. The interesting questions are, how does c_0 scale with q in the quasi-elastic limit, and what is the width of the crossover region? To address these questions, note that the series (4.13) converges for all velocities and the signs of the terms are alternating. Therefore, when breaking off the infinite sum at $n = N$, the maximum error is $|b_{N+1}|r_{N+1}$:

$$\begin{aligned} R(c) &= \sum_{n=0}^N b_n r_n + \Delta^{(N)}(c) \\ &\equiv R^{(N)}(c) + \Delta^{(N)}(c), \quad |\Delta^{(N)}(c)| \leq |b_{N+1}|r_{N+1}. \end{aligned} \quad (4.15)$$

This suggests that the pure exponential high energy tail $A_0 e^{-a|c|}$ qualitatively describe the large- c behavior of

$f(c)$ if

$$|b_1|r_1 = \frac{e^{-a|c|q/p}}{2q} \simeq \frac{e^{-\sqrt{q}|c|}}{2q} \leq \frac{1}{2}. \quad (4.16)$$

Of course the bound $\frac{1}{2}$ may be replaced by any number of the order of 1 in this estimate. Equation (4.16) implies that $w \equiv |c|\sqrt{q}/\ln q^{-1} \geq 1$. Therefore, we can estimate the crossover velocity to be $c_0 = (\ln q^{-1})/\sqrt{q}$ or, equivalently, $w_0 = 1$. To confirm this and get a closed form for the crossover function $R(c)$, consider a value of w in the range $0.5 < w < 1$ and take $N = \beta q^{w-1}$, where $\beta \gtrsim 1$. In that case, $N \gg 1$ but $N^2 q \ll 1$, so that $r_n \simeq q^{nw}$ and $b_n \simeq (-1)^n/n!(2q)^n$ for $n \lesssim N$, and $|b_{N+1}|r_{N+1} \simeq (2\beta/e)^{-N}/2\beta\sqrt{2\pi N}$. Therefore, with this choice of N ,

$$R^{(N)}(c) \simeq \sum_{n=0}^N \frac{(-1)^n}{n!} \left(\frac{q^{w-1}}{2} \right)^n, \\ |\Delta^{(N)}(c)| \leq \frac{1}{2\beta\sqrt{2\pi N}} \left(\frac{2\beta}{e} \right)^{-N}. \quad (4.17)$$

If $\beta > e/2 \simeq 1.36$ then $\Delta^{(N)}(c) \ll 1$ and $R(c)$ can be approximated by $R^{(N)}(c)$. By the same arguments, the upper limit in the summation of (4.17) can be replaced by infinity. The choice $N = \beta q^{w-1}$ is justified by the fact that for $w < 1$ the term $|b_n|r_n$ reaches a high maximum value $|b_{n_0}|r_{n_0} \simeq \exp(n_0 + \frac{1}{2})/\sqrt{2\pi n_0}$ at $n_0 \simeq \frac{1}{2}(q^{w-1} - 1)$ and then decays rapidly. If $w > 1$, however, $|b_n|r_n$ decreases monotonically and thus $\Delta^{(N)}(c) \ll 1$ for any choice of N . In conclusion, the crossover function for $w > 0.5$ in the quasi-elastic limit becomes

$$R(c) \simeq \exp(-q^{w-1}/2), \quad w \equiv |c|\sqrt{q}/\ln q^{-1}. \quad (4.18)$$

At $w = 1$ we have $R(c = c_0) \simeq 1/\sqrt{e} \simeq 0.6$, thus confirming the estimate of the crossover velocity c_0 made below Eq. (4.16). Figure 3 represents the crossover function $R(c)$ versus the scaled velocity w for $q = 0.01, 0.001, 0.0001$. To measure the width of the crossover region, let w_1 and w_2 denote the values of w at which $R = 0.1$ and $R = 0.9$, respectively. From Eq. (4.18) we obtain $w_1 \simeq 1 - 1.5/\ln q^{-1}$, $w_2 \simeq 1 + 1.6/\ln q^{-1}$, so the width scales as $w_2 - w_1 \sim 1/\ln q^{-1}$. Going back to unscaled velocities, the crossover takes place between $c_1 = c_0 - 1.5/\sqrt{q}$ and $c_2 = c_0 + 1.6/\sqrt{q}$ with a width $c_2 - c_1 \sim 1/\sqrt{q}$. For $q = 0.01, 0.001, 0.0001$ one has $c_0 \simeq 46, 218, 921$ and $c_2 - c_1 \simeq 31, 98, 310$, respectively. For these high values of the velocity the distribution function is extremely small. For instance, at $c = c_0$, $f(c_0) \simeq \frac{1}{2} \exp[(q^{-1} + \frac{1}{2}) \ln q + \pi^2/12q - K_0 - \frac{1}{2}]$. This yields $f(c_0) \sim 10^{-166}, 10^{-2645}, 10^{-36431}$ for $q = 0.01, 0.001, 0.0001$, respectively. These values are beyond the accuracy of any numerical or simulation method, so the high energy tail in the quasi-elastic limit would look like a Maxwellian for the domain of velocities numerically accessible. On the other hand, our asymptotic analysis of the exact solution shows that the true tail is actually exponential.

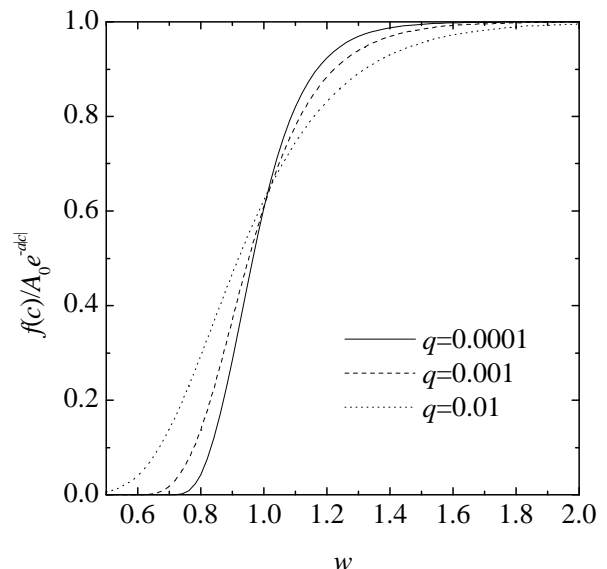


FIG. 3: Plot of the ratio between the velocity distribution function $f(c)$ and its high energy tail $A_0 e^{-a|c|}$ as a function of the scaled velocity $w \equiv |c|\sqrt{q}/\ln q^{-1}$ in the quasi-elastic limit for $q = 0.01, 0.001, 0.0001$.

V. CONCLUSION

The exact nonequilibrium steady state solution of the nonlinear Boltzmann equation for a driven one-dimensional inelastic Maxwell gas was obtained in Ref. [15] in the form of an infinite product for the Fourier transform $\phi(k)$ of the distribution function $f(c)$. The main goal of this paper has been to show that this relatively simple exact solution in the one-dimensional case also possesses the generic properties of overpopulation of high energy tails and exhibits a rich mathematical structure, especially in the different limiting cases.

We have inverted the Fourier transform to express $f(c)$ in the form of an infinite series of exponentially decaying terms, as given by Eq. (3.3) with the velocity c measured in units of the r.m.s velocity (i.e. $\langle c^2 \rangle^{1/2} = 1$). For all values of the coefficient of restitution $0 \leq \alpha < 1$ the high energy tail is exponential, namely $f(c) \simeq A_0 \exp(-a|c|)$, where $a \equiv 1/\sqrt{pq} = 2/\sqrt{1-\alpha^2}$ and the amplitude A_0 is given by Eq. (3.8) and plotted in Fig. 1.

Special attention has been paid to two complementary limiting cases: the totally inelastic limit ($\alpha \rightarrow 0$) and the quasi-elastic limit ($\alpha \rightarrow 1$). In the former case some poles coalesce and the dominant high energy term is still exponential, but the subdominant term becomes an exponential times a linear function of the velocity, where the numerical value of the associated amplitudes is given by (3.16).

The quasi-elastic limit is much more delicate and requires some care. If we first take $\alpha \rightarrow 1$ at fixed $|c|$ and next $|c| \rightarrow \infty$ (order A), the high energy tail has a Maxwellian form. On the other hand, if the limits are taken in the reverse order, i.e. first $|c| \rightarrow \infty$ at fixed $\alpha < 1$

and then $\alpha \rightarrow 1$ (order B), the asymptotic high energy tail is exponential. The crossover between both limiting behaviors is described by the coupled limit $c \rightarrow \infty$ and $q \rightarrow 0$ with the scaling variable $w = |c|\sqrt{q}/\ln q^{-1}$ fixed with $q \equiv \frac{1}{2}(1 - \alpha) \ll 1$, and occurs at $w \simeq 1$. If $w < 1$ (more specifically, $1 - w \gtrsim 1/\ln q^{-1}$), the distribution function is essentially a Maxwellian, while the true exponential high energy tail is reached if $w > 1$ (more specifically, $w - 1 \gtrsim 1/\ln q^{-1}$).

It is of interest to emphasize that the results for the scaling form in the quasi-elastic limit not only depend sensitively on the order in which both limits are taken. They also depend strongly on the collisional interaction, i.e. on the energy dependence of the collisional frequency, as well as on the mode of energy supply to the system. To illustrate this we have collected in Table I what is known for the different inelastic models in one dimension: (i) hard spheres and (ii) Maxwell models, and for different modes of energy supply: (i) no energy input or free cooling, (ii) energy input or driving through Gaussian white noise, represented by the forcing term $-D\partial^2 F(v, t)/\partial v^2$ in the Boltzmann equation, and (iii) energy input through a *negative* friction force $\propto gv/|v|$, acting in the direction of the particle's velocity, but independent of its speed. This driving, referred to as gravity thermostat, can be represented as the forcing term $g(\partial/\partial v)[(v/|v|)F(v, t)]$ in the Boltzmann equation. The results corresponding to order A with the gravity thermostat have been obtained by the same method as followed in Ref. [8]. It is worthwhile noting that in the quasi-elastic limit a bimodal distribution, $\frac{1}{2}[\delta(c+1) + \delta(c-1)]$, is observed in inelastic hard sphere systems both for free cooling and for driving through the gravity thermostat, whereas in inelastic Maxwell models this bimodal distribution is only observed for the gravity thermostat.

It is important to note that in the normalization where velocities are measured in units of the r.m.s. velocity, the high energy tail in the driven inelastic Maxwell model is only observable for very large velocities, as illustrated in Figure 2 for strong ($\alpha \rightarrow 0$) and intermediate ($\alpha = \frac{1}{2}$) inelasticity. In the quasi-elastic limit, where ($\alpha \rightarrow 1$), the tail is even pushed further out towards infinity, as analyzed at the end of Section IV. This also explains how to reconcile the paradoxical results of exponential large- c behavior with the very accurate representation (4.4) of the distribution function in the thermal range, in the form of a Maxwellian, multiplied by a polynomial expansion in Hermite or Sonine polynomials with coefficients related to the cumulants. The validity of these polynomial expansions, over a large range of inelasticities with ($0 \leq \alpha < 1$) had been observed before in [5] for inelastic hard spheres and in [18] for inelastic Maxwell models. On the other hand the high energy tail is $\propto e^{-a|c|}$, and not $\propto c^N e^{-c^2/2}$, where N is some large number, and yields diverging moments $M_{2n} = \langle c^{2n} \rangle$ and cumulants C_{2n} in the limit $n \rightarrow \infty$, as shown in Section II.

The exact solutions of the nonlinear Boltzmann equa-

tion for the freely evolving [13] and the driven [15] inelastic Maxwell model (extended in this paper), as well as the rigorous proof of [24] for the long time approach of the distribution function to a scaling form, validate the self consistent method, developed in [5] for analytical studies of possible over- or underpopulations of the high energy tail of velocity distributions, not only for inelastic Maxwell models, but – more importantly – also for inelastic hard sphere, where exact solutions are not known. This possibility of assessing the validity of general kinetic theory methods by means of exact solutions of the nonlinear Boltzmann equation is one of the main reasons why the study of inelastic Maxwell models is of interest.

Acknowledgments

The authors are indebted to B. Nienhuis for stimulating discussions about the subject of this paper. A.S. acknowledges partial support from the Ministerio de Ciencia y Tecnología (Spain) through grant No. BFM2001-0718.

APPENDIX A: LARGE- k EXPANSION

The asymptotic behavior of ψ for large k can be obtained by inserting the ansatz, $\psi = -\lambda|k| + \ln(Ak^2) + \sum_{n=1}^{\infty} a_n k^{-2n}$, with unknown coefficients $\{A, a_n\}$ into (2.2), and equating the coefficients of equal powers of $\ln k$ and k^n with the result,

$$\psi(k) = -\lambda|k| + \ln(k^2/pq) - \sum_{n=1}^{\infty} \frac{(-1)^n}{n} \frac{(k^2 pq)^{-n}}{p^{-2n} + q^{-2n} - 1}, \quad (\text{A1})$$

where λ is as yet undetermined. The series converges for $k^2 \geq q/p$. However for the $\psi(k)$ above to qualify as a solution of (2.2) the radius of convergence is further restricted to $(qk)^2 \geq q/p$ or $pqk^2 \geq 1$. The constant λ must be chosen such that $\psi(k)$ satisfies the boundary condition $\psi \simeq -\frac{1}{2}k^2$ at small k . This can be done by matching (A1) with (2.4). The latter satisfies already the small- k boundary condition. Matching at $pqk^2 = 1$ yields then,

$$\begin{aligned} \frac{\lambda}{\sqrt{pq}} &= -2 \ln(pq) + \sum_{n=1}^{\infty} \frac{(-1)^{n+1}}{n} \\ &\times \left(\frac{1}{1-p^{2n}-q^{2n}} + \frac{1}{p^{-2n}+q^{-2n}-1} \right). \end{aligned} \quad (\text{A2})$$

Both terms can be combined into a single n -sum with $n = \pm 1, \pm 2, \dots$. The above result is not only convenient for numerical evaluation, as shown in Fig. 4, but also for analytic evaluation in two limiting cases. We first consider the *totally inelastic* limit ($\alpha \rightarrow 0$ or $p = q = \frac{1}{2}$).

TABLE I: Asymptotic behavior of the distribution function $f(c)$ for one-dimensional systems in the quasi-elastic limit. In general, the result depends on the order of limits. Order A corresponds to take first $\alpha \rightarrow 1^-$ and then $|c| \rightarrow \infty$, whereas order B refers to the reverse order, i.e. first $|c| \rightarrow \infty$ and then $\alpha \rightarrow 1^-$. The first/second footnote in the second column gives the reference where the result for order A/B was obtained.

| State | System | Order A | Order B |
|--------------------|------------------------------|---|-------------------|
| Free cooling | Hard spheres ^{a,b} | $\frac{1}{2} [\delta(c-1) + \delta(c+1)]$ | $e^{-a c }$ |
| | Maxwell model ^{c,c} | c^{-4} | c^{-4} |
| White noise | Hard spheres ^{a,d} | $e^{-a c ^3}$ | $e^{-a c ^{3/2}}$ |
| | Maxwell model ^{e,f} | e^{-ac^2} | $e^{-a c }$ |
| Gravity thermostat | Hard spheres ^{e,g} | $\frac{1}{2} [\delta(c-1) + \delta(c+1)]$ | e^{-ac^2} |
| | Maxwell model ^{e,h} | $\frac{1}{2} [\delta(c-1) + \delta(c+1)]$ | $e^{-a c }$ |

^aRef. [8]

^bRef. [5]

^cRefs. [13, 15, 22]

^dRefs. [5, 8]

^eThis work

^fRefs. [8, 23]

^gRef. [10]

^hRef. [23]

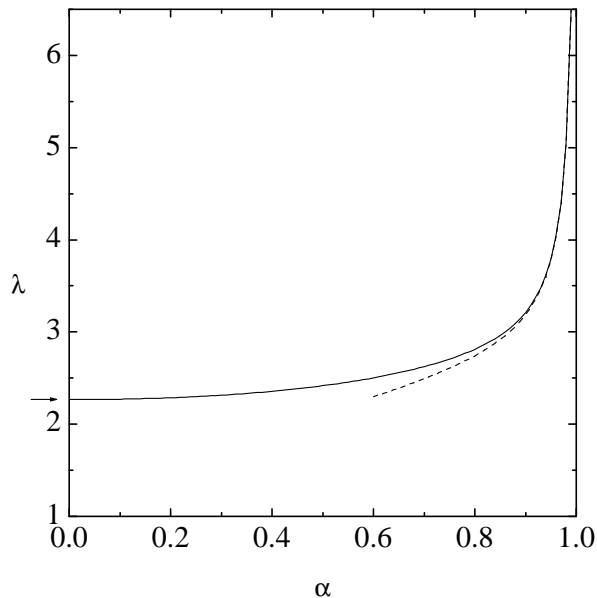


FIG. 4: Coefficient λ as a function of the coefficient of restitution. The arrow indicates the value $\lambda = \pi/2 \ln 2$ at $\alpha = 0$. The dotted line represents the asymptotic form Eq. (A7) for small q .

There the expansion (A1) can be cast into a simpler form,

$$\begin{aligned}
 \psi(k) &= -\lambda|k| + \ln(4k^2) - \frac{1}{2} \sum_{n=1}^{\infty} \frac{(-1)^n}{n} \frac{k^{-2n}}{1-2^{-(2n+1)}} \\
 &= -\lambda|k| + \ln(4k^2) + \frac{1}{2} \sum_{m=0}^{\infty} \frac{1}{2^m} \ln\left(1 + \frac{1}{2^{2m}k^2}\right) \\
 &= -\lambda|k| + \frac{1}{2} \sum_{m=0}^{\infty} \frac{1}{2^m} \ln(1 + 2^{2m}k^2). \quad (\text{A3})
 \end{aligned}$$

Matching this expression in $k^2 = 1/pq = 4$ with the exact solution in (2.3), $\psi(2) = -\sum_{m=0}^{\infty} 2^m \ln(1 + 2^{-2m})$, yields

the nice result,

$$\begin{aligned}
 \lambda &= \frac{1}{2} \sum_{m=-\infty}^{\infty} 2^m \ln(1 + 2^{-2m}) \\
 &= \frac{1}{4 \ln 2} \int_0^{\infty} dx x^{-3/2} \ln(1+x) = \frac{\pi}{2 \ln 2}. \quad (\text{A4})
 \end{aligned}$$

One can verify using the Euler–MacLaurin summation formula (see Eq. (23.1.30) of [29]) that all correction terms to the integral are vanishing, and the integral is listed in Eq. (4.293.3) of [30].

In the *quasi-elastic* limit ($\alpha \rightarrow 1$ or $q \rightarrow 0$) the sum originating from the second term inside (\dots) in (A2) is of $\mathcal{O}(q^2)$, and will be neglected. To evaluate the first term T for small q we expand it as follows,

$$\begin{aligned}
 T &= \sum_{k=1}^{\infty} \frac{(-1)^{k+1}}{k} \frac{1}{1-p^{2k}} \left[1 + \frac{q^{2k}}{1-p^{2k}} + \mathcal{O}(q^{2(2k-1)}) \right] \\
 &= \sum_{k=1}^{\infty} \frac{(-1)^{k+1}}{k} \left[\frac{1}{2kq} + \frac{2k-1}{4k} + \frac{q^{2k}}{(2kq)^2} + \mathcal{O}(q) \right] \\
 &= -\frac{1}{2q} \text{Li}_2(-1) - \frac{1}{2} \text{Li}_1(-1) + \frac{1}{4} \text{Li}_2(-1) + \frac{1}{4} + \mathcal{O}(q), \quad (\text{A5})
 \end{aligned}$$

where the polylogarithmic functions are defined as,

$$\text{Li}_k(x) = \sum_{n=1}^{\infty} x^n / n^k \quad (\text{A6})$$

with $\text{Li}_2(-1) = -\frac{1}{12}\pi^2$ and $\text{Li}_1(-1) = -\ln 2$ [31]. The final result for λ at small q is then,

$$\begin{aligned}
 \lambda &= \frac{1}{\sqrt{q}} \left[\frac{\pi^2}{24} - 2q \ln q + \frac{1}{2} q (\ln 2 + \frac{1}{2} - \frac{\pi^2}{12}) \right. \\
 &\quad \left. + q^2 \ln q + \mathcal{O}(q^2) \right]. \quad (\text{A7})
 \end{aligned}$$

**APPENDIX B: ASYMPTOTICS IN
QUASI-ELASTIC LIMIT**

To calculate $B_n^{(3)}$ in (4.7) for small q we expand the logarithm, and perform the (m, ℓ) -summation. The result is,

$$\begin{aligned} B_n^{(3)} &= \sum_{k=1}^{\infty} \frac{p^{2k}}{k(1-p^{2k})} \frac{(1+q^{2k}/p^{2k})^{n+1}}{1-q^{2k}/(1-p^{2k})} \\ &= \sum_{k=1}^{\infty} \frac{p^{2k}}{k(1-p^{2k})} \left[1 + \frac{q^{2k}}{1-p^{2k}} + \frac{q^{4k}}{(1-p^{2k})^2} + \frac{(n+1)q^{2k}}{p^{2k}} \right] + o(q) \\ &\equiv S(x) + \delta S(n, x) + o(q), \end{aligned} \quad (\text{B1})$$

where all contributions $\propto q^0$ and $\propto q$ have been included. The dominant term is,

$$S(x) = \sum_{k=1}^{\infty} \frac{e^{-kx}}{k(1-e^{-kx})} \quad (x = -2 \ln p). \quad (\text{B2})$$

In the remaining contributions to (B1) only the term $k = 1$ needs to be taken into account, and yields

$$\delta S(x, n) = \frac{1}{4} + \frac{1}{2}q(n + \frac{3}{4}) \simeq \frac{1}{4} + \frac{1}{4}x(n + \frac{3}{4}). \quad (\text{B3})$$

To study the small- x behavior of (B2) we construct an asymptotic series for $S(x)$, by expanding $1/(1-e^{-kx})$ in powers of x . This can be done most conveniently by using the small- x expansion of $x \coth x$, or equivalently the generating function for the Bernoulli numbers, $B_{2k} = (-1)^{k+1} |B_{2k}|$ (see Eqs (23.1.1-2) of [29]), which we write as,

$$\frac{1}{1-e^{-x}} = \frac{1}{x} + \frac{1}{2} + \sum_{m=1}^{\infty} \frac{B_{2m}}{(2m)!} x^{2m-1}. \quad (\text{B4})$$

Substitution of (B4) with $x \rightarrow kx$ into (B2) yields,

$$\begin{aligned} S(x) &= \frac{1}{x} \text{Li}_2(e^{-x}) - \frac{1}{2} \ln(1-e^{-x}) \\ &+ \sum_{m=1}^{\infty} \frac{x^{2m-1}}{(2m)!} B_{2m} \text{Li}_{2-2m}(e^{-x}). \end{aligned} \quad (\text{B5})$$

We have used the definition (A6) of the polylogarithmic functions, which are all singular in $x = 0$. To determine the behavior of the dilogarithm, $\text{Li}_2(e^{-x})$ we use the functional relation (see Eq. (5) of [31]),

$$\begin{aligned} \text{Li}_2(e^{-x}) &= \frac{\pi^2}{6} - \ln(e^{-x}) \ln(1-e^{-x}) - \text{Li}_2(1-e^{-x}) \\ &= \frac{\pi^2}{6} + x(\ln x - \frac{1}{2}x) - (x - \frac{1}{4}x^2) + \mathcal{O}(x^3). \end{aligned} \quad (\text{B6})$$

Here the small- x expansion of the sum in (B5) can be obtained from the relation,

$$\begin{aligned} \text{Li}_{-n}(e^{-x}) &= \sum_{k=1}^{\infty} k^n e^{-kx} \\ &= \left(-\frac{d}{dx}\right)^n \text{Li}_0(e^{-x}) = \left(-\frac{d}{dx}\right)^n (e^x - 1)^{-1} \\ &= \left(-\frac{d}{dx}\right)^n \left\{ \frac{1}{x} - \frac{1}{2} + \sum_{m=1}^{\infty} \frac{B_{2m}}{(2m)!} x^{2m-1} \right\} \\ &= \frac{n!}{x^{n+1}} \left[1 - \frac{1}{2}x\delta_{n0} + o(x) \right]. \end{aligned} \quad (\text{B7})$$

The small- x expansion of $1/(e^x - 1)$ has been obtained from (B4) with $x \rightarrow -x$.

By combining the relations (B6) and (B7) with the small- x expansion of $\ln(1-e^{-x})$, we obtain from (B5),

$$\begin{aligned} S(x) &= \frac{\pi^2}{6x} + \frac{1}{2} \ln(1-e^{-x}) - \frac{1}{x} \text{Li}_2(1-e^{-x}) \\ &+ \sum_{m=1}^{\infty} \frac{B_{2m}}{2m(2m-1)} \left(1 - \frac{1}{2}x\delta_{m1}\right) \\ &= \frac{\pi^2}{6x} + \frac{1}{2} \ln x - 1 + R_0 - \frac{x}{24} + \mathcal{O}(x^2), \end{aligned} \quad (\text{B8})$$

where $R_0 \equiv \sum_{m=1}^{\infty} B_{2m}/[2m(2m-1)]$. As $|B_{2k}| \sim 2(2k)!/(2\pi)^{2k}$ for $k \rightarrow \infty$ (see Eqs. (23.2.16) and (23.2.18) of [29]), the series is a divergent asymptotic series with *alternating* signs. One obtains the greatest accuracy, denoted by $R_0^{(m_0)}$, if one breaks off the series just before the smallest term in the series, which is defined to be the $(m_0 + 1)$ -th term. Then the maximum error is $|B_{2m_0+2}/(2m_0+1)(2m_0+2)|$ (see Chap. 0.33 of [30]). In the present case one can simply verify that $m_0 = 3$, and the best possible estimate for the remainder in the limit where $q \rightarrow 0$ is given by,

$$R_0 = R_0^{(3)} \pm \frac{1}{56} |B_8| \simeq 0.0813492 \pm 0.0005952. \quad (\text{B9})$$

The inaccuracy in $S(x)$, caused by the inaccuracy in the asymptotic series R_0 , can be substantially reduced – if so desired – by restricting the m -sum in (B5) to $m_0 = 3$ terms, and calculating the difference,

$$\begin{aligned} \Delta(x) &= \sum_{k=1}^{\infty} \frac{e^{-kx}}{k} \left[\frac{1}{1-e^{-kx}} - \frac{1}{kx} - \frac{1}{2} \right. \\ &\quad \left. - \sum_{m=1}^3 \frac{B_{2m}}{(2m)!} (kx)^{2m-1} \right], \end{aligned} \quad (\text{B10})$$

in the small- x limit as an integral. The result for instance, to seven decimal points is $\Delta = -0.0002877$. Hence

$$R_0 = R_0^{(3)} + \Delta \simeq 0.0810615. \quad (\text{B11})$$

Combination of the results (B1), (B3) and (B8) gives the dominant small- x behavior of $B_n^{(3)}$ in the form,

$$B_n^{(3)} = \frac{\pi^2}{6x} + \frac{1}{2} \ln x - \frac{3}{4} + R_0 + \frac{1}{4}x(n + \frac{7}{12}). \quad (\text{B12})$$

Final elimination of $x = 2q(1 + \frac{1}{2}q + \frac{1}{3}q^2 + \dots)$ in favor of q gives (4.9) in the main text.

-
- [1] A. V. Bobylev, Sov. Phys. Dokl. **20**, 820 (1976); M. Krook and T. T. Wu, Phys. Rev. Lett. **36**, 1107 (1976); M. H. Ernst, Phys. Rep. **78**, 1 (1981).
- [2] D. R. M. Williams and F. C. MacKintosh, Phys. Rev. E **54**, R9 (1996).
- [3] D. R. M. Williams, Physica A **233**, 718 (1996).
- [4] S. E. Esipov and T. Pöschel, J. Stat. Phys. **86**, 1385 (1997).
- [5] T. P. C. van Noije and M. H. Ernst, Gran. Matt. **1**, 57 (1998) and cond-mat/980342.
- [6] M. R. Swift, M. Boamfã, S. J. Cornell, and A. Maritan, Phys. Rev. Lett. **80**, 4410 (1998).
- [7] C. Bizon, M. D. Shattuck, J. B. Swift, and H. L. Swinney, Phys. Rev. E **60**, 4340 (1999).
- [8] A. Barrat, T. Biben, Z. Rácz, E. Trizac, and F. van Wijland, J. Phys. A: Math. Gen. **35**, 463 (2002).
- [9] J. J. Brey, M. J. Ruiz-Montero, and D. Cubero, Phys. Rev. E **54**, 3664 (1996).
- [10] J. M. Montanero and A. Santos, Gran. Matt. **2**, 53 (2000) and cond-mat/0002323.
- [11] T. P. C. van Noije, M. H. Ernst, E. Trizac, and I. Pagonabarraga, Phys. Rev. E **59**, 4326 (1999); I. Pagonabarraga, E. Trizac, T. P. C. van Noije and M. H. Ernst, Phys. Rev. E **65**, 011303 (2002).
- [12] G. P. Collins, Sci. Am. **284**(1), 17 (2001); F. Rouyer and N. Menon, Phys. Rev. Lett. **85**, 3676 (2000); D. L. Blair and A. Kudrolli, Phys. Rev. E **64**, 050301(R) (2001); I. S. Aranson and J. S. Olafsen, Phys. Rev. E **66**, 061302 (2002).
- [13] A. Baldassarri, U. Marini Bettolo Marconi, and A. Puglisi, Europhys. Lett. **58**, 14 (2002).
- [14] A. Baldassarri, U. Marini Bettolo Marconi, and A. Puglisi, Phys. Rev. E **65**, 051301 (2002).
- [15] E. Ben-Naim and P. L. Krapivsky, Phys. Rev. E **61**, R5 (2000).
- [16] S. Ulam, Adv. Appl. Math. **1**, 7 (1980).
- [17] A. V. Bobylev, J. A. Carrillo, and I. M. Gamba, J. Stat. Phys. **98**, 743 (2000); see also erratum: J. Stat. Phys. **103**, 1137 (2001).
- [18] J. A. Carrillo, C. Cercignani, and I. M. Gamba, Phys. Rev. E **62**, 7700 (2000).
- [19] M. H. Ernst and R. Brito, in: *Theory of Granular Gases*, Lecture Notes in Physics (Springer-Verlag, Berlin), T. Pöschel and N. Brilliantov, eds., to be published.
- [20] E. Ben-Naim and P. L. Krapivsky, in: *Theory of Granular Gases*, see [19], and cond-mat/0301238.
- [21] P. L. Krapivski and E. Ben-Naim, J. Phys. A: Math Gen. **35**, L147 (2002).
- [22] M. H. Ernst and R. Brito, Europhys. Lett. **58**, 182 (2002); J. Stat. Phys. **109**, 407 (2002).
- [23] M. H. Ernst and R. Brito, Phys. Rev. E **65**, 040301(R) (2002).
- [24] A. V. Bobylev, C. Cercignani, and G. Toscani, J. Stat. Phys. **111**, 403 (2003).
- [25] B. Nienhuis and R. van der Hart, unpublished; R. van der Hart, *Road Models and Granular Gases*, Master's thesis, Universiteit van Amsterdam, May 24, 2002.
- [26] U. Marini Bettolo Marconi and A. Puglisi, Phys. Rev. E **66**, 011301 (2002).
- [27] T. Antal, M. Droz, and A. Lipowski, Phys. Rev. E **66**, 062301 (2002).
- [28] The normalization chosen here is the same as in [13]. In Refs. [22, 23, 26] the normalization is $\langle c^2 \rangle = 1/2$ and $D = \frac{1}{2}pq$ when specialized to a one-dimensional system, and in Refs. [25, 27] one has $\langle c^2 \rangle = 1/pq$ and $D = 1$.
- [29] M. Abramowitz and I. Stegun, *Handbook of Mathematical Functions* (Dover, New York, 1972).
- [30] I. S. Gradshteyn and I. M. Ryzhik, *Table of Integrals, Series, and Products* (Academic Press, New York, 1980).
- [31] See <http://mathworld.wolfram.com/Polylogarithm.html> and [/Dilogarithm.html](http://mathworld.wolfram.com/Dilogarithm.html).